Journal of
Chemical Engineering & Process Technology

Fakhri and Adami, J Chem Eng Process Technol 2013, 4:5
DOI: 10.4172/2157-7048.1000161

Research Article Open Access

Response Surface Methodology for Adsorption of Fluoride Ion Using Nanoparticle of Zero Valent Iron from Aqueous Solution

Ali Fakhri* and Saeideh Adami

Department of Chemistry, Shahre-Qods Branch, Islamic Azad University, Tehran, Iran

Abstract

This study is removal of fluoride ion from aqueous solution by nano zero valent iron (nZVI). Effects of the factor variables (temperature, nZVI dose and pH) and their interactions on adsorption of fluoride ion were investigated by response surface methodology (RSM) based on Box-Behnken design (BBD). Optimized values of temperature, nZVI dose and pH for fluoride sorption were found as 313K, 0.5 g, and 4, respectively. The effect of initial fluoride concentration on the adsorption amount was investigated by a batch experiment. For study the fluoride removal mechanism, various adsorption isotherms such as Langmuir, Freundlich and Temkin were fitted. The results showed that the Freundlich isotherm gave high fit for fluoride adsorption. The time of adsorption reaction was rapid and subordinated pseudo-second-order kinetics. The values of thermodynamic parameters indicated that adsorption was spontaneous and endothermic in nature. The nano zero valent iron (nZVI) could be used as a potential adsorbent for fluoride ion containing aqueous solution.

Keywords: Adsorption; Fluoride; Box-Behnken design; Nanoparticle zero valent iron; Response surface methodology

Introduction

Fluoride is a health affecting substance. The physiologic effects of fluoride ingestion on public health have been studied extensively [1]. The acceptable fluoride concentration in drinking water is generally in the range of 0.5 to 1.5 mgl^{-1} [2]. High concentration has the effects on the metabolism of elements such as Ca, P in human body and lead to dental and skeletal fluorosis. The fluoride content of soils varies from under 20 to several thousand ppm, the higher records being mostly from areas with bedded phosphate on fluoride deposits [3]. The natural presence of fluoride generally occurs through soil and rock formation in the form of fluorapatite, fluorspar and amphiboles, geochemical deposits, natural water systems and earth crust [4,5]. In addition to this fluoride can also be found in various Industrial work, chiefly semiconductor, electroplating, glass, steel, ceramic and fertilizers industries [6]. Because of these reasons the pollution of ground water by fluoride contamination has been a major concern. The problems in connection with fluoride ion pollution could be reduced or minimized by ultra-filtration, precipitation, reverse osmosis, electrode-deposition, etc., but these processes have flaws such as high cost, generation of secondary pollutants and low removal efficiency. Adsorption experiment has been found to be an effective and economic method with high potential for the removal, recovery and recycle of fluoride ions from aqueous solution [7], although desorption is an issue.

Zero valent iron (ZVI) was proposed as a reactive material in permeable reactive barriers (PRGs) due to its great ability in reducing and the stabilization pollutants different [8]. Nowadays, there has been an increasing interest in synthesizing this material on nanoscale for to enhance its ability restore by probity of the increase in the surface area and surface reactivity of the particles [9]. Nano zero valent iron (nZVI), a recently discovered technology, is being used to successfully treatment various organic compounds (e.g. [10-12]) and various heavy metal ions in aqueous solutions (e.g. [13-18]).

Design of experiments (DOE) and response surface methodology (RSM) is largely used for modeling mechanism parameters, especially in adsorption or removal process [19-32]. Because RSM contains a lower number of experiments, it is flaws over conventional methods available. It is suitable for multi-factor experiments and searches the common connection between various factors for the determined of most favorable or unfavorable conditions of the processes. Response surface methodology has different model types such as central composite design (CCD), Doehlert matrix (DM) and Box-Behnken design (BBD). The objective of this study was the application of the RSM combined with Box-Behnken design as a statistic method in optimizing adsorption mechanism of fluoride ion using nano zero valent iron. The Langmuir, Freundlich and Temkin isotherm models were used to define the equilibrium data. The adsorption mechanisms of fluoride ion from aqueous solutions onto nZVI were also evaluated in terms of kinetics and thermodynamic parameters.

Materials and Methods

Raw materials

Sodium fluoride salt (NaF) (molecular weight, 41.98871 g/mol) was supplied by Merck Co. (Germany) (maximum purity available > 99%). Doubly distilled deionized water (HPLC grade 99.99% purity) was obtained from Sigma Aldrich Co. (Germany).

Synthesis of nanoparticle zero valent iron (nZVI)

The nZVI material was synthesized by drop wise addition of 1.6 M NaBH4 (sodium borohydride) aqueous solution to a Ne gas-purged 1 M $FeCl_3.6H_2O$ (Ferric chlorid hexahydrate) aqueous solution at 23°C with magnetic stirring as described by Wang and Zhang [33]. Ferric iron (Fe^{3+}) was reduced according to the reaction [34]: $4Fe^{+3} + 3BH_4 + 9H_2O \rightarrow 4Fe^0 + 3H_2BO_3^- + 12H^+ + 6H_2$.

***Corresponding author:** Ali Fakhri, Department of Chemistry, Shahre-Qods Branch, Islamic Azad University, Tehran, Iran, Tel: +98(21)22873079; Fax: +98(21)22873079; E-mail: ali.fakhri88@yahoo.com

Received April 18, 2013; **Accepted** June 12, 2013; **Published** June 14, 2013

Citation: Fakhri A, Adami S (2013) Response Surface Methodology for Adsorption of Fluoride Ion Using Nanoparticle of Zero Valent Iron from Aqueous Solution. J Chem Eng Process Technol 4: 161 doi:10.4172/2157-7048.1000161

The solution was stirred for 20 min and centrifuged at 6000 rpm for 2 min, and the supernatant solution was replaced by acetone. Acetone-washing prevented the immediate rusting of nZVI during purification leading to a fine black powder product after freeze-drying. X-ray diffractometer (XRD, Philips X'Pert) was used to investigate the material structure of zero valent iron nanoparticles. In addition, the surface morphology of nZVI was determined using transmission electron microscopy (TEM, JEM-2100F HR, 200 kV).

Adsorption experiment

The adsorption of fluoride onto nZVI was investigated using batch experiments. In these studies 1000 mg/L stock solution was prepared by dissolving 1 g of NaF in 1000 mL distilled water. Different concentrations (20-200 mg/L) of fluoride solutions were prepared by this stock solution. Solutions were evacuated to flasks of 100 ml. Then adsorbent in the range of dosage 0.05-0.5 g was added and placed in the water bath shaker after pH adjustments made in the range of 2-10. The suspensions were shaken at 2000 rpm for 12 min at room temperature. Samples from shaker were filtered with filter paper, and then remaining fluoride levels were measured using a fluoride electrode (Orion, 9606BNWP). The final adsorption amount was calculated from the equation $q_e = \frac{(C_o - C_e)V}{W}$ (1)

where, qe (mg/g) is the equilibrium adsorption amount, C_e is the fluoride concentration at equilibrium (mg/l), V is the volume of solution (l) and w is the weight of adsorbent (g).

Response surface methodology

The three-level, three-factorial Box-Behnken experimental design with categorical factor of 0 was engaged to optimize the treatment process based on the adsorption amount of the nZVI for fluoride ion. The design was composed of three levels (low, medium and high, being coded as (-1, 0 and +1) and a total of 17 runs were carried out in repetitious to optimize the level of chosen variables, such as temperature, nZVI dosage and pH. For the aim of statistical calculations, the three factor variables were denoted as x_1, x_2, and x_3, respectively. According to the preparatory experiments, the range and levels used in the experiments are selected and listed in Table 1. The main effects and in connection between factors were determined. Figure 1 illustrates the mean of the experimental results for the respective low, medium and high levels of temperature, pH and nZVI dosage of scattering. The experimental design matrix by the Box-Behnken design is tabulated in table 2 and corresponding experiments were performed. The results were analyzed by applying the response plots and analysis of variance (ANOVA). For RSM, the most commonly used second-order polynomial equation developed to fit the experimental data can be written as:

$$Y = \beta_0 + \sum_{i=1}^{k} \beta_i x_i + \sum_{i=1}^{k} \beta_{ii} x_i^2 + \sum_{1 \le i \le j}^{k} \beta i_j x_i x_j + \varepsilon \quad (2)$$

where Y represents the predicted response, i.e. the adsorption amount

Factor	Low level (-1)	Medium level (0)	High level (+1)
Temperature (X_1)	283 K	297 K	313 K
nZVI dosage (X_2)	0.25 g	0.50 g	0.75 g
pH (X_3)	4	8	12

Table 1: Factors and levels used in the factorial design.

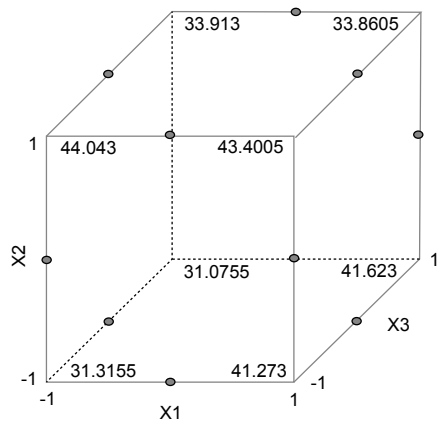

Figure 1: Cube plots for Y.

Runs	X_1	X_2	X_3	Y_{Exp} (mg/g)
1	0	0	0	22.48
2	0	0	0	22.55
3	+1	+1	0	30.84
4	+1	0	-1	45.20
5	0	0	0	22.53
6	0	0	0	22.38
7	-1	0	1	31.39
8	-1	+1	0	32.37
9	+1	0	+1	37.82
10	-1	-1	0	25.24
11	0	-1	-1	25.48
12	0	+1	+1	26.51
13	0	0	0	22.43
14	0	+1	-1	33.56
15	-1	0	-1	39.36
16	0	-1	+1	28.32
17	+1	-1	0	34.31

Table 2: BBD and results for the study of three experimental variables in coded units.

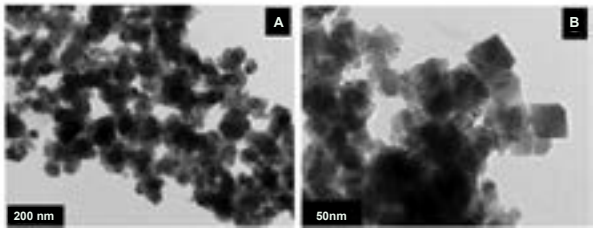

Figure 2: TEM images of (A) nZVI and (B) nZVI after adsorption of fluoride ion.

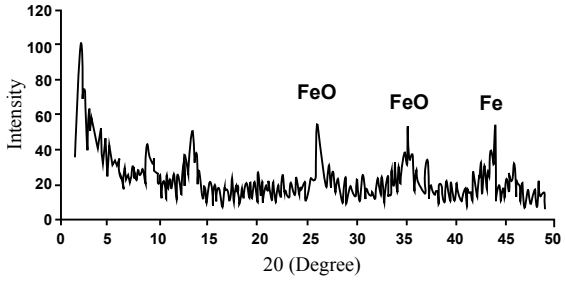

Figure 3: X-Ray diffraction pattern of Nanoparticle zero valent iron (nZVI) surface.

for fluoride ion by the nZVI (mg/g), β_0, the constant coefficient, β_i, the i^{th} linear coefficient of the input factor x_i, β_{ii}, the i^{th} quadratic coefficient of the input factors x_i, β_{ij}, the different interaction coefficients between input factors x_i and x_j (i = 1–3, j = 1–3 and i / = j), and ε, the error of the model [35]. The equation expresses the in connection between the predicted response and factor variables in coded values according to Tables 1 and 2.

Results and Discussion

Characterization of nZVI

Figure 2 shows the transmission electron microscope image of freshly synthesized iron nanoparticles. Surface morphology shows that there exist two layers in the nZVI particle. The layer of intrant core Indicative the Fe^0, and the external layer surrounding on the Fe^0 was iron-oxide(s). Figure 2B shows that the fluoride molecules into the nZVI surface are covered. The X-Ray diffraction of nZVI surface composition under ambient conditions is shown in Figure 3. The wide peak reveals the being of an amorphous phase of iron. The characteristic broad peak at 2θ of 45° indicates that the zero valent iron is predominantly present in the sample.

Statistical analysis

The optimum terms for adsorption of fluoride onto nZVI surface were determined by means of the BBD under RSM. The results were displayed in Tables 3. In this manner, the fluoride uptake by nZVI could be described using the following equation: $Y = 22.474 + 2.476\ X_1 + 1.241\ X_2 - 2.445\ X_3 - 2.650\ X_1X_2 + 0.147\ X_1X_3 - 2.472\ X_2X_3 + 9.095\ X_{12} - 0.879\ X_{22} + 6.873\ X_{23}$ (3)

The state of the fitted model was declared by the coefficient of determination. The R^2 coefficient gives the relation of the total variation in the response predicted by the model and a high R^2 value (close to 1) is desirable. Eq. (3) Indication that the model is well fitted, considering the determination coefficient (R^2= 97.71%). The estimated effects and coefficients for model are listed in Table 3. Model terms were evaluated by the P-value (probability) with 95% confidence level. The P-values were used to estimate whether F was large enough to indicate statistical significance and used to check the significance of each coefficient. The P-values lower than 0.05 indicated that the model and model terms were statistically significant. All the factors and their square interactions (P < 0.05) except for interaction of temperature–temperature (X_1^2) and pH-pH (X_3^2) were significant at the 95% confidence level. nZVI dose was the most significant factor that affect the removal of fluoride. Also, the quadratic effect of nZVI dose - nZVI dose (X_2^2) was found larger than effect of nZVI dose, and the removal of fluoride significantly decreased. Figure 4 shows that the data were well distributed near to a straight line (R^2=0.9726), which proposed a good relationship between the experimental and predicted values of the response, and the underlying assumptions of the above analysis were appropriate.

Source	Sum of Squares	df	Mean Square	F Value	p-value Prob > F
Model	738.36	9	82.04	29.94	<0.0001
Temperature(X_1)	49.05	1	49.05	17.90	0.0039
nZVI dosage (X_2)	12.33	1	12.33	4.50	0.0716
pH (X_3)	47.82	1	47.82	17.45	0.0041
Temperature-nZVI dosage (X_1X_2)	28.09	1	28.09	10.25	0.0150
Temperature-pH (X_1X_3)	0.087	1	0.087	0.032	0.8636
nZVI dosage-pH (X_2X_3)	24.45	1	24.45	8.92	0.0203
Temperature-Temperature (X_1^2)	348.33	1	345.33	127.13	<0.0001
nZVI dosage- nZVI dosage (X_2^2)	3.26	1	3.26	1.19	0.3117
pH-pH (X_3^2)	198.90	1	198.90	72.59	<0.0001
Residual	19.18	7	2.74		
Lack of Fit	19.16	3	6.39		
Pure Error	0.020	4	4.930E-003		
Cor Total	757.55	16			

Table 3: Analysis of variance for the response of the adsorption capacity for fluoride ion.

3D response surface plot

The 3D response surface plot are useful in investigation both the main and interaction effects of the factors [36,37]. The response surface plots are presented in Figure 5. This figure also shows the estimated Y parameter as a function of the normalized factor variables, the height of the surface represents the value of Y. After executing a screening of factors using a BBD, the surface plots of the response (Y) indicated the same results as observed in the interaction plot (Figure 5).

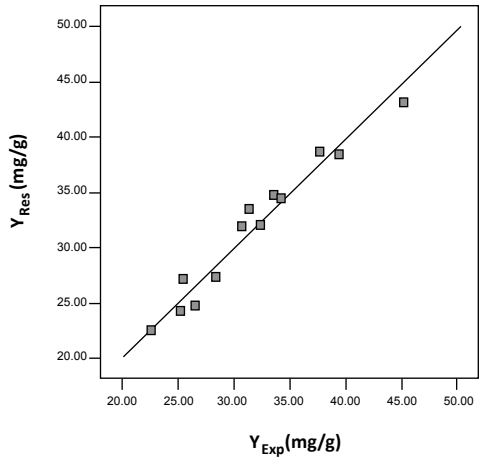

Figure 4: Plot of the experimental and predicted responses.

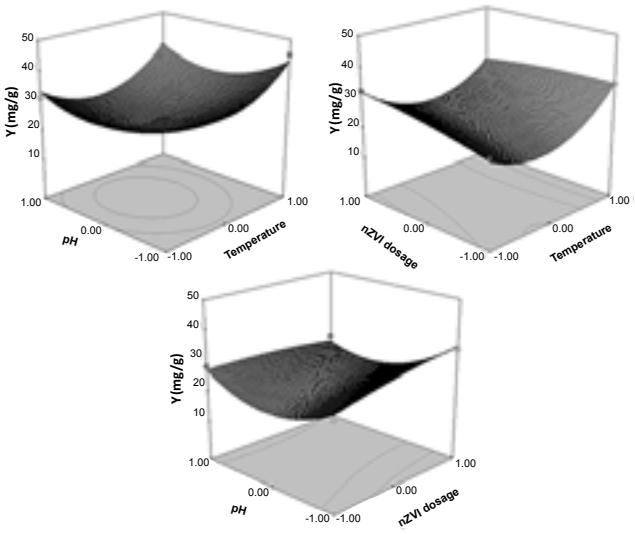

Figure 5: Response surface plots of adsorption capacity versus the effect of three variables.

Adsorption isotherms

The mechanism of fluoride adsorption from aqueous solutions onto nZVI is evaluated using adsorption isotherm. In this study, isotherm data were applied to four adsorption models and the results of their linear regressions were used to find the model with the best fit. Values of resulting parameters and regression coefficients (R^2) are listed in Tables 4 and 5.

The R^2 value for the Freundlich isotherm was 0.9990, which is higher than the values obtained from the Langmuir and Temkin isotherm models. The experimental data fit very well to this isotherm model, and indicates that fluoride adsorption occurs on heterogeneous surfaces, which is similar to the conclusion reached for nZVI [38-40].

Adsorption kinetics

Various models have been used to investigation of the adsorption mechanisms and potential rate. Effects of contact time on adsorption are investigated, as shown in Figure 6. The adsorption process was quite rapid and reached equilibrium in 30 min (Figure 6). In this study, the different kinetics models such as pseudo-first-order, pseudo-second-order, and intra-particle diffusion models were used.

Isotherm model	Equation
Langmuir	$\frac{C_e}{q_e}=\frac{1}{K_L q_m}+\frac{C_e}{q_m}$
Freundlich	$ln\,q_e = ln\,K_F + \frac{1}{n} ln\,C_e$
Temkin	$q_e = B_1 \ln K_T + B_1 \ln C_e$

Table 4: Summary of equilibrium isotherms (K_L, K_F, B_1, K_T: Langmuir, Freundlich and Temkin constants; n: heterogeneity coefficient; q_m: maximum adsorption capacity; q_e: uptake at equilibrium; C_e: equilibrium concentration; b: activity coefficient related to mean sorption energy).

Langmuir model			
K_L(L/g)	q_m(mg/g)		R^2
0.1053	129.87		0.9902
Freundlich			
K_F(mg/g)/(mg/L)$^{1/n}$	n		R^2
14.2235	1.4212		0.9990
Temkin			
K_T(L/mg)	B_1	b=RT/B_1	R^2
1.1161	27.943	88.367	0.9876

Table 5: Langmuir, Freundlich and Temkin isotherm constants for adsorption of Fluoride ion.

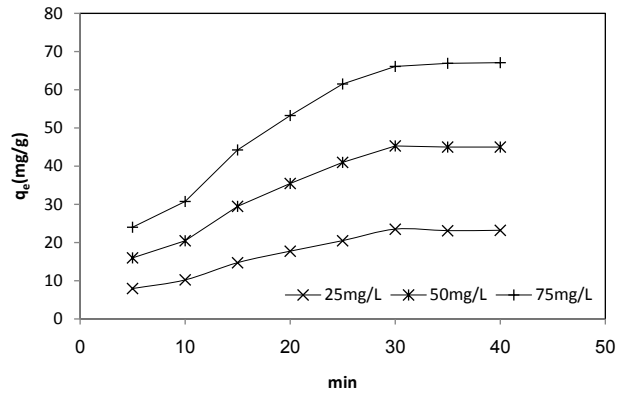

Figure 6: Optimisation of contact time for fluoride removal (initial pH: 4.0; adsorbent dose: 0.5 g/L).

The pseudo-first-order rate equation is given as [41]: $\log (q_e - q_t) = \log (q_e) - \left(\frac{k_1}{2.303}\right) t$ (4)

where q_e and q_t are the amounts of fluoride adsorbed (mg/g) at equilibrium and at time t (min), respectively, and k_1(L/min) is the adsorption rate constant of first-order adsorption. A straight line of $\log(q_e-q_t)$ versus t (Figure not shown) suggests the applicability of this kinetic model. q_e and k_1 were determined from the intercept and slope of the plot which were shown in Table 6. From the data, q_e (calculated) and q_e (experimental) values are not in agreement with each other. Therefore, that indicates the adsorption of fluoride on nZVI was not a first-order reaction.

In addition, the experimental data was also applied to the pseudo-second-order kinetic model Equation [42]:

$$\frac{t}{qt}=\frac{1}{k_2 q_e^2}+\frac{t}{q_e} \quad (5)$$

where k_2 is the rate constant of pseudo-second-order chemisorptions (g/(mg min)). The plot t/q_t versus t giving a straight line which is shown in Figure 7 and the constant calculated from the slop and intercept of the plots are given in Table 6. Figure 7 shows that R^2 values are higher than those obtained from the first-order kinetics. In addition, theoretical and experimental q_e values are in agreement. Therefore, it is

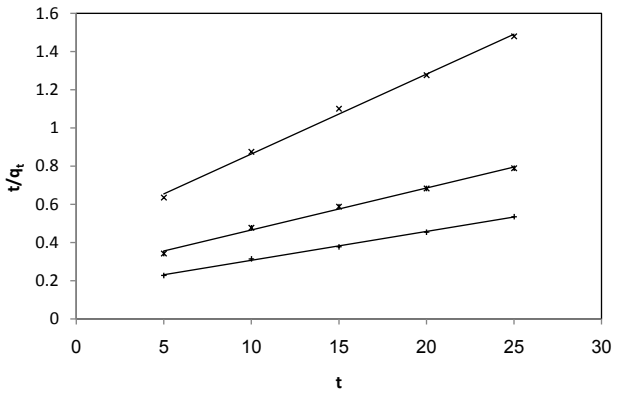

Figure 7: Second-order kinetic plot for fluoride adsorption on nZVI at different initial concentration.

Fluoride ion concentration (mg/L)	25	50	75
$q_{e,exp}$ (mg/g)	23.50	45.31	66.12
Pseudo-first-order model			
q_e (mg/g)	20.73	25.85	36.71
k_1 (min^{-1})	0.0291	0.0301	0.0302
R^2	0.9826	0.9801	0.9828
Pseudo-second-order model			
q_e (mg/g)	23.92	45.45	66.22
k_2 ($g.mg^{-1}.min^{-1}$)	0.0039	0.0019	0.0014
R^2	0.9967	0.9957	0.9981
Intra-particle diffusion model			
k_i ($mg.g^{-1}.min^{-1}$)	4.8227	9.4463	13.871
C	3.7547	6.8723	9.3529
R^2	0.9843	0.9850	0.9841

Table 6: Kinetic parameters and experimental adsorption capacities for fluoride onto nZVI.

possible to prove that the adsorption process using nZVI followed the second-order kinetic model.

The intra-particle diffusion equation can be described as:

$$q = k_i t^{1/2} + C \quad (9)$$

where ki is the intra-particle diffusion rate constant (mg/g min). The data (Figure not shown) shown have an initial curved portion, followed by a linear portion. The curved portion of the plot is due to the diffusion of fluoride through the solution to the external surface of nZVI, or boundary layer diffusion. However, the extrapolated linear regions at different initial concentrations did not pass through the origin and that suggests that the intra-particle diffusion was not the rate-controlling step [43].

Thermodynamic of adsorption studies

Thermodynamic parameters connected to the adsorption reaction, i.e., Gibbs free energy change (ΔG°, kJ mol^{-1}), enthalpy change (ΔH°, kJ mol^{-1}), and entropy change (ΔS°, J mol^{-1} K^{-1}) are defined by the following equations: $\Delta G° = -RT\ln Kc$ (8)

$$\Delta G° = \Delta H° = \Delta H° - T\Delta S° \quad (9)$$

where K_c is the equilibrium constant, which can be obtained from Langmuir isotherm, R is the universal gas constant, 8.314 $Jmol^{-1}$ K^{-1}, and T is absolute temperature (K). ΔH° and ΔS° were obtained from the slope and intercept of the plot of Gibbs free energy change, ΔG° vs. temperature, T (Figure 8).

The negative values of ΔG ° (-5.746, -6.793 and -8.270 KJ mol^{-1} for 283, 297 and 313K, respectively) confirm the feasibility of the process and the spontaneous nature of adsorption with a high preference for fluoride onto nZVI. The standard enthalpy and entropy changes determined from plot in Figure 8. The value of ΔH° is positive (18.165 KJ mol^{-1}), indicating that the adsorption reaction is endothermic. The positive value of ΔS° (84.300 J $mol^{-1}K^{-1}$) reflects an increase in the randomness at the solid/solution interface during the adsorption process [44].

Conclusions

The statistical design of the experiments was applied in optimizing the conditions of maximum adsorption of the fluoride onto nZVI. The result data from ANOVA demonstrates that the model was highly significant. nZVI dose was the most significant factor affecting fluoride removal. Therefore, it is apparent that the response surface methodology not only gives valuable information on interactions between the factors but also helps to the recognition of possible optimum values of the studied factors. Adsorption experiments show that the adsorption equilibrium can be achieved within 30 min. The kinetics studies of fluoride on nZVI indicated that the adsorption kinetics of fluoride on nZVI followed the pseudo-second order at different initial concentration. The results of Isotherm data showed that the removal of fluoride followed Freundlich isotherm. Thermodynamic adsorption studies indicated that the adsorption fluoride using nZVI aqueous solution was a spontaneous, endothermic.

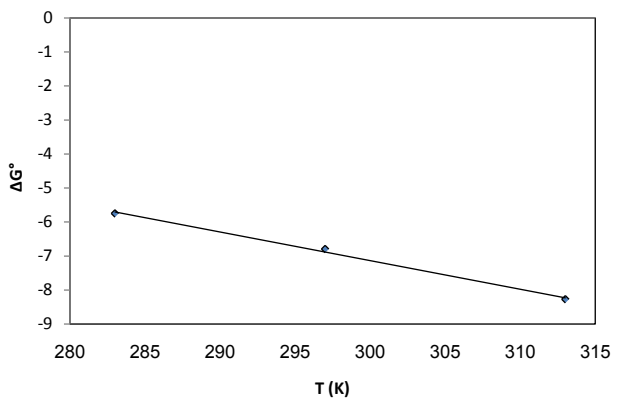

Figure 8: Plot of Gibbs free energy change vs. temperature for fluoride ion adsorption onto nZVI.

Acknowledgment

The authors gratefully acknowledge supporting of this research by the Islamic Azad University Shahre-Gods Branch.

References

1. Zhu CS, Bai GL, Liu XL, Li Y (2006) Screening high-fluoride and high-arsenic drinking waters and surveying endemic fluorosis and arsenic in Shaanxi province in western China Water Research. 40: 3015-3022.
2. WHO (2008) Guidelines for Drinking Water Quality, World Health Organization, Geneva.
3. Bishnoi M, Arora S (2007) Potable groundwater quality in some villages of Haryana, India: Focus on fluoride J Environ Biol 28: 291-294.
4. Shailaja K, Johnson MEC (2007) Fluorides in groundwater and its impact on health. J Environ Biol 28: 331-332.
5. Tripathy SS, Bersillon JL, Gopal K (2006) Removal of fluoride from drinking water by adsorption onto alum-impregnated activated alumina. Sep Purif Technol 50: 310-317.
6. Toyoda A, Taira A (2000) IEEE Trans, Semiconductor Manufacture. 13: 305-309.
7. Bailey SE, Olin TJ, Bricka RM, Adrian DD (1999) A review of potentially low-cost sorbents for heavy metals. Water Res 33: 2469-2479.
8. Blowes DW, Ptacek CJ, Benner SG, McRae Che WT, Bennett TA, et al. (2000) Treatment of inorganic contaminants using permeable reactive barriers. J Contam Hydrol 45: 123-137.
9. Sun Y, Li X, Cao J, Zhang W, Wang HP (2006) Characterization of zero-valent iron nanoparticles. Adv Colloid Interf Sci 120: 47-56.
10. Liu Y, Majetich SA, Tilton RD, Sholl DS, Lowry GV (2005) TCE dechlorination rates, pathways, and efficiency of nanoscale iron particles with different properties. Environ Sci Technol 39: 1338-1345.
11. Joo SH, Feitz AJ, Sedlak DL, Waite TD (2005) Quantification of the oxidizing capacity of nanoparticulate zero-valent iron. Environ Sci Technol 39: 1263-68.
12. Li XQ, Brown DG (2007) Zhang WX, Stabilization of biosolids with nanoscale zero-valent iron (nZVI). J Nanoparticle Res 9: 233.
13. Li XQ, Zhang WX (2007) Sequestration of metal cations with zerovalent iron nanoparticles-a study with high resolution X-ray photoelectron spectroscopy (HR-XPS). J Phys Chem 111: 6939-6946.
14. Uzum C, Shahwan T, Eroglu AE, Hallam KR, Scott TB, et al. (2009) Synthesis and characterization of kaolinite-supported zero-valent iron nanoparticles and their application for the removal of aqueous Cu2+ and Co2+ ions. Appl Clay Sci 43: 172-181.
15. Elebi OC, Uzum C, Shahwan T, Erten HNA (2007) A radiotracer study of the adsorption behavior of aqueous Ba2+ ions on nanoparticles of zero-valent iron. J Hazard Mater 148: 761-767.
16. Kanel SR, Manning B, Charlet L, Choi H (2005) Removal of arsenic (III) from groundwater by nanoscale zero-valent iron. Environ Sci Technol 39: 1291-1298.
17. Jegadeesan G, Mondal K, Lalvani SB (2005) Arsenate remediation using nano sized modified zero valent iron particles. Environ Prog 24: 289-296.
18. Li XQ, Zhang WX (2006) Iron nanoparticles: the core–shell structure and unique properties for Ni(II) sequestration. Langmuir 22: 4638-4642.

19. Kaushik P, Malik A (2011) Process optimization for efficient dye removal by Aspergillus lentulus FJ172995. J Hazard Mater 185: 837-843.

20. Ghorbani F, Younesi H, Ghasempouri SM, Zinatizadeh AA, Amini M, et al. (2008) Application of response surface methodology for optimization of cadmium biosorption in an aqueous solution by Saccharomyces cerevisiae. Chem Eng J 145: 267-275.

21. Abdel-Ghani NT, Hegazy AK, El-Chaghaby GA, Lima EC (2009) Factorial experimental design for biosorption of iron and zinc using Typha domingensis phytomass. Desalination 249: 343-347.

22. Cestari AR, Vieira EFS, Oliveira IA, Bruns RE (2007) The removal of Cu(II) and Co(II) from aqueous solutions using cross-linked chitosan-Evaluation by the factorial design methodology. J Hazard Mater 143: 8-16.

23. Hasan SH, Srivastava P, Talat M (2009) Biosorption of Pb(II) from water using biomass of Aeromonas hydrophila: Central composite design for optimization of process variables. J Hazard Mater 168: 1155-1162.

24. Annadurai G, Juang RS, Lee DJ (2002) Factorial design analysis for adsorption of dye on activated carbon beads incorporated with calcium alginate. Advances in Environmental Research 6: 191-168.

25. Ravikumar K, Krishnan S, Ramalingam S, Balu K (2007) Optimization of process variables by the application of response surface methodology for dye removal using a novel adsorbent. Dyes Pigments 72: 66-74.

26. Cestari AR, Vieira EFS, Mota JA (2008) The removal of an anionic red dye from aqueous solutions using chitosan beads-The role of experimental factors on adsorption using a full factorial design. J Hazard Mater 160: 337-343.

27. Bingol D, Tekin N, Alkan M (2010) Brilliant Yellow dye adsorption onto sepiolite using a full factorial design. Applied Clay Science 50: 315-321.

28. Jabasingh SA, Pavithra G (2010) Response Surface Approach for the Biosorption of Cr6+ Ions by Mucor racemosus. CLEAN-Soil, Air, Water 38: 492-499.

29. Zolgharnein J, Shahmoradi A, Sangi MR (2008) Optimization of Pb(II) biosorption by Robinia tree leaves using statistical design of experiments. Talanta 76: 528-532.

30. Zolgharnein J, Adhami Z, Shahmoradi A, Mousavi SN, MR Sangi (2010) Multivariate optimization of Cd(II) biosorption onto Ulmus tree leaves from aqueous waste. Toxicological and Environmental Chemistry 8: 1461-1470.

31. Bingöl D (2011) Removal of Cadmium (II) from Aqueous Solutions using a Central Composite Design. Fresenius Environmental Bulletin 10: 2704-2709.

32. Das D, Das N (2011) Response Surface Approach for the Bisorption of Ag(I) by Macro fungus Pleurotus platypus. CLEAN – Soil, Air, Water 2: 157-161.

33. Wang CB, Zhang W (1997) Synthesizing nanoscale iron particles for rapid and complete dechlorination of TCE and PCBs. Environ. Sci. Technol. 31: 2154-2156.

34. Glavee GN, Klabunde KJ, Sorensen CM, Hadjipanayis GC (1995) Chemistry of borohydride reduction of iron(II) and iron(III)ions in aqueous and nonaqueous media. formation of nanoscale Fe, FeB, and Fe2B powders. Inorg Chem 34: 28-35.

35. Benyounis KY, Olabi AG, Hashmi MSJ (2005) Effect of laser welding parameters on the heat input and weld-bead profile. J Mater Process Technol 164: 978-980.

36. Cojocaru C, Trznadel GZ (2007) Response surface modeling and optimization of copper removal from aqua solutions using polymer assisted ultrafiltration. J Membr Sci 298: 56-70.

37. Arbizu IP, Luis Pérez CJ (2003) Surface roughness prediction by factorial design of experiments in turning processes. J Mater Process Technol 143: 390-396.

38. Ponnusami V, Krithika V, Madhuram R, Srivastava SN (2007) Biosorption of reactive dye using acid-treated rice husk: factorial design analysis. J Hazard Mater 142: 397-403.

39. Mathialagan T, Viraraghavan T (2005) Biosorption of pentachlorophenol by fungal biomass from aqueous solutions: a factorial design analysis. Environ Technol 6: 571-579.

40. Sujana MG, Thakur RS, Rao SB (1998) Removal of fluoride from aqueous solution by using alum sludge. J Colloid Inter Sci 206: 94-101.

41. Lagergren S (1898) About the theory of so called adsorption of soluble substances. Vetenskapsad Handl 24: 1-39.

42. Ho YS, Mckay G (1999) Pseudo-second order model for sorption process Process Biochem 34: 451-465.

43. Gupta VK, Ali I, Saini VK (2007) Defluoridation of wastewaters using waste carbon slurry. Water Res 41: 3307-3316.

44. Ngah WSW, Fatinathan S (2008) Adsorption of Cu(II) ions in aqueous solution using chitosan beads, chitosan-GLA beads and chitosan-alginate beads. Chem Eng J 143: 62-72.